LA-UR-76-1425

CONF-760914--1

TITLE: INSENSITIVE EXPLOSIVE STUDIES USING PHERMEX

AUTHOR(S): Richard D. Dick

SUBMITTED TO: American Society for Nondestructive Testing
Flash X-ray Symposium, Houston, Texas,
September 27-30, 1976.

los alamos
scientific laboratory
of the University of California
LOS ALAMOS, NEW MEXICO 87544

An Affirmative Action/Equal Opportunity Employer

Form No. 836
St. No. 2629
1/75

UNITED STATES
ENERGY RESEARCH AND
DEVELOPMENT ADMINISTRATION
CONTRACT W-7405-ENG. 36

INSENSITIVE EXPLOSIVE STUDIES USING PHERMEX*

by

Richard D. Dick

University of California
Los Alamos Scientific Laboratory
Los Alamos, New Mexico 87545

Abstract

Flash radiographs were obtained of insensitive explosives (mixtures of TATB explosive and Kel-F binder) of several shapes using the PHERMEX flash X-ray facility at the Los Alamos Scientific Laboratory. The purpose was to examine radiographically the corner-turning ability of an insensitive explosive, the character of the expanding detonation wave from a spherical initiation, and the characteristics of colliding detonation waves. A comparison of certain aspects of the corner-turning properties of the insensitive explosive is made with a sensitive explosive (Composition B). Measurements from the radiographs are used to calculate a C-J pressure and a γ value for the insensitive explosives and these are compared to data from sensitive explosives.

Introduction

Vigorous experimental and theoretical programs to understand the behavior of insensitive and sensitive explosives are in progress at the Los Alamos Scientific Laboratory.

*Work performed under the auspices of the Energy Research and Development Administration

Some areas of study of insensitive explosives are the following: models for the detonation process, measurements of detonation around a corner, detonation spreading from a localized initiation, and effects of colliding detonation waves. The role of PHERMEX is to obtain flash radiographs from which quantitative measurements can be obtained and which also provide a unique opportunity to see the phenomena of interest in perspective. This paper describes several PHERMEX experiments pertinent to the insensitive explosive program.

X-0219 and X-0290 Explosives

The insensitive explosives under study are two different mixtures of TATB (triaminotrinitrobenzene) explosive and Kel-F binder. They are designated X-0219 (90% TATB/10% Kel-F) and X-0290 (95% TATB/5% Kel-F). Both are solid with a density of about 1.9 Mg/m^3 and are readily pressed and machined. Both explosives are very difficult to detonate and require the use of a booster of sensitive explosive such as a layer of Composition B or 9404 for initiation. Once full detonation begins it is self-sustaining with a specific energy release comparable to that of Composition B.

Corner-Turning Experiments

An important property of an explosive in practical applications is the ability of the detonation wave to turn a corner and propagate unabated. In a sensitive explosive such as Composition B the detonation front can turn a sharp corner with little or no loss in energy release.[1] This is not the case, however, for insensitive explosives like X-0219 and X-0290.[2] A series of flash radiographic experiments has been performed to observe the corner-turning or divergence capability and the existence of an unreacted zone in X-0219 and X-0290.

Figure 1 is a cross-section view of a typical shot assembly including the setup-dimensions, and the position of the PHERMEX beam axis (BAX). The explosive charge was L-shaped with 90° corners and was 146 mm thick. A Lucite plate cemented to the explosive served as a mechanical support and as a means for determining some of the explosive parameters. Detonation of the insensitive explosive was accomplished by a P/081 plane wave explosive lens and a 9404 explosive booster. Each shot was positioned so that the PHERMEX machine beam axis was near the location of the anticipated unreacted zone, which was left behind after the detonation wave had propagated past the 90° corner. Dynamic radiographs were taken at different times to follow the progress of the detonation front as it propagated beyond the corner.

The X-ray target-to-shot center distance was 1.83 m and shot center-to-film distance was 1.22 m resulting in a radiographic magnification of 1.67. A conical film protector contained the film package which was composed of combinations of Kodak AA and KK industrial X-ray film and 1-mm-thick lead screens. Figure 2 is a schematic drawing of the experimental setup at the firing point. For these experiments the X-ray pulse duration was 40 ns with radiation levels of 10 to 20 R measured in air at 1 m.

A reproduction of a typical dynamic radiograph from the experiments containing X-0219 is shown in Fig. 3. The time of this radiograph was 45.04 μs measured from application of the trigger voltage to the firing set. The times for the other experiments are listed in Table I.

The distinguishing features (see Fig. 3) of the radiographs are the curved and well-defined detonation front in X-0219, the large triangular-shaped zones (light area on the photograph) of compressed explosive, the sharply defined boundary between the compressed zone and the explosive gases on the side toward the corner, the complex circular gas flow pattern connected to the dense zone, the presence of a slightly curved shock wave in the Lucite, and the slanted front and back surfaces of the Lucite plate. Less obvious features are the gradual increase in film density (decrease in material density) as the eye proceeds left from the dense spot into the gaseous region and the rarefaction front extending back into the detonation products.

A radiograph of a shot using X-0290 is shown in Fig. 4. The detonation characteristics are similar to those of X-0219 except the size of the compressed spot is considerably smaller in X-0290.

An interpretation of the behavior of the insensitive explosives from these corner-turning experiments is as follows. As the detonation front propagates past the right angle, a compressed and probably unreacted zone begins to build. This zone changes size, shape, and location as time progresses. This is illustrated in the composite drawings of Figs. 5 and 6. The size and area of the zone are listed in Table I. The detonation front, which originally was at the apex of the triangular shaped zone, travels down the side of the triangle leaving behind the isolated region of unreacted but compressed explosive. It appears that the zone has advanced to the right from the corner at a velocity of

about 2.6 km/s in X-0219 and 2.2 km/s in X-0290. These zones seem to persist as undetonated regions for many microseconds after formation and may never detonate in the normal sense.

Measurements of the average detonation velocities from the time sequenced radiographs illustaated in Figs. 5 and 6 indicate a 13% decrease in velocity in X-0219 from the normal value of 7.53 km/s and a 20% decre .e from the normal velocity of 7.63 km/s in X-0290. These percentages are not precise but the trend suggests a reduction in pressure after the detonation front turns through an angle of about 45°. There is a significant difference between X-0219 and X-0290 in the distance between the leading part of the detonation wave and the position of the wave at the air-explosive interface after detachment from the unreacted zones. This is also shown in Figs. 5 and 6.

Some measurements from the radiographs were used to provide a more quantitative description of the behavior of X-0219 and X-0290. Some measurements and calculational results are listed in Table I. The angles α and θ listed in Table I are defined in Figs. 5 and 6. The column heading "t, ℓ, h, and area" are the radiographic time, distance of the apex of the triangular spot from the 90° corner, the height of the spot, and the approximate area of the compressed region. From a measurement of the angle θ from the radiographs, the shock speed (U_s) in the Lucite is determined from the equation

$$U_s = D \sin \theta \quad ,$$

where D is the known detonation velocity in the explosive. Then from the known Hugoniot of the Lucite, defined[3] by

$$U_s = 2.26 + 1.82\, U_p \text{ and } \rho_o = 1.18 \text{ Mg/m}^3,$$

the pressure (P), particle velocity (U_p), and density (ρ) for the Lucite are calculated. These values are listed in Table I. The angle α associated with the Lucite back surface could be measured from the radiographs but a more precise value can be calculated from the equation[4]

$$\frac{\rho_o}{\rho} = \frac{\tan(\theta-\alpha)}{\tan\theta} \quad ,$$

where ρ_o and ρ are the initial and final density of the Lucite. Once α and the pressure in the Lucite are known, the Chapman-Jouguet (C-J) pressure of each insensitive explosive was calculated[4] from a gamma-law analysis[5] for an explosive. The basic equation is

$$E = \frac{P}{\rho(\gamma-1)} - Q \quad ,$$

where E and ρ are the energy and density, respectively, behind the detonation front, γ is a constant for the explosive, and Q is the energy release from the detonation reaction. The calculational procedure is to choose a value for γ that reproduces the measured pressure in the Lucite and the angle α, given the detonation velocity and the initial density of the explosive. The value of γ determined in this manner is not very accurate because the measurement of θ is not precise and because the shock impedances of the explosive and Lucite are poorly matched. The calculated values for γ, the detonation pressure (C-J pressure), and other parameters for the two insensitive explosives are compared in Table II with some data for several sensitive explosives.[6,7]

Divergence Experiments with Aluminum in the Corner

Some experiments in which a detonation wave propagates past a 90° corner containing aluminum were conducted using X-0219 and X-0290 explosive.

This arrangement is similar to experiments[8] conducted several years ago with Composition B. The experimental setup is illustrated in Fig. 7. A P/081 lens simultaneously sent a shock wave into the aluminum block and detonated the explosive. A radiograph was taken after the detonation front traveled around the corner and interacted with a low amplitude shock wave transmitted into the explosive from the aluminum.

The radiographic geometry was 4.1 m from the target to the shot and 0.9 m from shot to film, making the radiographic magnification 1.22. The film package consisted of a Kodak AA film between two 1-mm-thick lead screens, double lead-screened Kodak AA and KK films, and a single 1-mm-thick lead screen in front of a KK film. The package was protected in a conical film cassette. For this series of shots a radiation pulse width of 100 ns was used providing about 25 R at 1 m.

Figure 8 is a schematic drawing of the more important discontinuities from typical radiographs involving 90° aluminum corners. As illustrated an essentially straight detonation wave curves downward and meets the low amplitude shock wave (estiamted to be 5 GPa) in the explosive. A fan-shaped interaction region of (probably undetonated) explosive compressed by about 8 GPa of pressure extends toward the corner from the intersecting waves. Also shown on the schematic are reflected shock waves and a spall plane in the aluminum that are observed on the radiograph. The radiograph of the shot with a configuration identical to that for Fig. 8 but using X-0290 shows the same features except the interaction zone is slightly smaller.

Figure 9 is a reproduction of a radiograph from one of the previous tests using Composition B. Figure 10 is a radiograph from an

experiment using X-0219 and is shown here for comparison to Fig. 9. The features of the two radiographs are similar except the undetonated zone created by the interaction of the detonation wave and shock wave in Composition B is confined to a small area in the vicinity of the intersection (see Fig. 9). This is in contrast to the large unreacted zones in X-0219 (and in X-0290) extending back into the explosive (see Fig. 10). It also appears that a reaction has occurred in Composition B in the space behind the shock wave but not in the insensitive explosives.

Colliding Detonation Waves

These experiments were to provide radiographic data of the interaction zone produced by the collision of detonation waves after turning 90° along curved sections of X-0219 and X-0290 explosive. A diagram of the experiments is shown in Fig. 11. The ends of the U-shaped explosive were detonated simultaneously using P/081 lenses and booster charges. The radiograph was timed to occur about 500 ns after the detonation waves collided at the top. A target-to-shot distance of 1.83 m and the shot-to-film distance of 1.22 m was used for all the shots. The film package, film cassette, and processing were similar to those in the corner-turning experiments.

Figure 12 is a reproduction of a shot using X-0219 explosive featuring the collision zone. Unfortunately, the radiographic time was 0.5 to 1.0 μs too late and, consequently, some of the expected details were lost. The important features to be noted in Fig. 12 are the sharp boundries of the shock waves proceeding back into the explosive gases after collision and the seemingly constant density behind the two fronts

except for the formation of rarefaction waves in the lower part of the collision zone. In addition the outward expanding gases and the shock wave resulting from the gases converging toward the center of the area are observable.

A similar experiment using X-0290 is shown in Fig. 13. In this test the time was adjusted to provide a radiograph about 100 ns after collision. The images on the radiograph are the two shock waves reflecting back into the gases after collision producing a high pressure region between the two fronts, the detonation waves before collision, and an undetonated region. Also observable are the outward expanding detonation gases, the converging gases, and a rarefaction wave behind the detonation waves.

There were no large or abrupt material density changes between the two shock waves preceding into the explosive gases except for the rarefaction waves moving away from the symmetry plane. In addition there were no high-velocity jets attributed to the collision process and in general there were no surprises in the character of the collision zones.

Summary

The usefulness of the PHERMEX machine was again demonstrated by the quality of the radiographs and the image detail on the film in the study of the explosives reported in this paper. This form of flash radiography has provided direct observation of detonation processes characteristic of insensitive (and sensitive) explosives that were previously only conjecture. With more extensive analyses of the radiographs, quantitative data concerning areal mass distribution, precise definition of edges and discontinuities, and equation-of-state parameters can be determined. The experiments discussed in the text represent several of many possible approaches to the study of explosives. Some conclusions resulting from the experiments are listed below.

From the corner-turning experiments the conclusions are as follows: (1) In the open corner experiments on X-0219 and X-0290 a zone of compressed but undetonated explosive is created by the detonation wave sweeping past the 90° corner. The size of this unreacted region is about ten times larger for X-0219 than for X-0290 suggesting that X-0290 has the better corner-turning ability. As detonation progresses around the corner the detonation front separated and moved away from the unreacted zone leaving the zone completely enveloped by the explosive products. The zone retains its shape and approximate size and seems to persist for many microseconds. (2) The detonation velocities in X-0219 and X-0290 decrease significantly as the front turns the corner indicating a reduction in detonation pressure. (3) With aluminum in the corner the interaction in X-0219 and X-0290 of the detonation wave and a low amplitude shock wave transmitted from the aluminum into the explosive created a large and well defined unreacted zone. Similar studies with Composition B explosive indicate that only a small or no unreacted zone is formed at the interaction point. (4) The detonation pressures for X-0219 and X-0290 are approximately the same and both are comparable to Composition B.

The radiographs of the colliding detonation wave experiments revealed no unusual behavior.

References

1. W. C. Davis, Los Alamos Scientific Laboratory, private communication, 1975.
2. A. W. Campbell, W. C. Davis, J. B. Ramsey, and J. R. Travis, Los Alamos Scientific Laboratory, unpublished data, 1975.
3. "Selected Hugoniots," Los Alamos Scientific Laboratory report LA-4167-MS, 1969.
4. T. Neal, "Perpendicular Explosive Drive and Oblique Shocks," Proceedings Sixth Symposium (International) on Detonation, U. S. Government Printing Office, Washington, D. C., 1976, to be published.
5. H. M. Sternberg and D. Piacesi, "Interaction of Oblique Detonation Waves with Iron," Physics of Fluids, Vol. 9, 1966, p. 1307.
6. W. E. Deal, "Measurement of Chapman-Jouguet Pressure for Explosives," Journal of Chemical Physics, Vol. 27, 1951, p. 796.
7. G. E. Duval and G. R. Fowles, "Shock Waves," High Pressure Physics and Chemistry, Vol. 2, 1962, pp. 209-291, Academic Press.
8. D. Venable and R. W. Taylor, Los Alamos Scientific Laboratory, unpublished data, 1966.

TABLE I

SOME RESULTS FROM THE X-0219 AND X-0290 BOOT EXPERIMENTS

Shot No.	θ (deg)	t (μs)	ℓ (mm)	h (mm)	Area (mm²)
	X-0219 (D = 7.53 km/s and ρ_0 = 1.914 Mg/m³)				
1071	47.06	43.98	12.6	13.8	120
1082	45.61	45.04	13.8	12.0	120
1078	-	46.04	15.5	12.0	90
	X-0290 (D = 7.63 km/s and ρ_0 = 1.892 Mg/m³)				
1079	46.15	41.00	3.0	7.8	14
1072	46.49	43.72	9.9	4.6	14
1083	46.71	44.49	10.8	3.6	10

	Lucite					Compressed Zone	
HE	α (deg)	U_s (km/s)	U_p (km/s)	P (GPa)	ρ (Mg/m³)	Mass (g)	V[a] (km/s)
X-0219	10.98	5.45	1.76	11.3	1.74	33	2.6
X-0290	11.10	5.53	1.80	11.8	1.75	4	2.2

[a]Speed of the unreacted zone from the 90° corner.

TABLE II

COMPARISON OF X-0219 AND X-0290 INSENSITIVE EXPLOSIVE WITH OTHER EXPLOSIVES

Oblique Detonation Induced Pressures (GPa)

	Al	Cu	H_2O	Lucite
Composition B	18.9	20.5	12.1	10.5
X-0219				11.3
X-0290				11.8

Explosive Parameters

HE	ρ_0 (Mg/m^3)	ρ_{CJ} (Mg/m^3)	P_{CJ} (GPa)	U_{CJ} (km/s)	D (mm/s)	γ
TNT	1.637	2.153	18.9	1.664	6.942	3.172
Composition B	1.713	2.331	29.2	2.127	8.018	2.770
Cyclotol	1.743	2.366	31.3	2.173	8.252	2.798
RDX	1.767	2.375	33.8	2.213	8.637	2.904
X-0219	1.914	2.70	31.7	2.20	7.53	2.43
X-0290	1.892	2.70	32.9	2.28	7.63	2.36

List of Figures

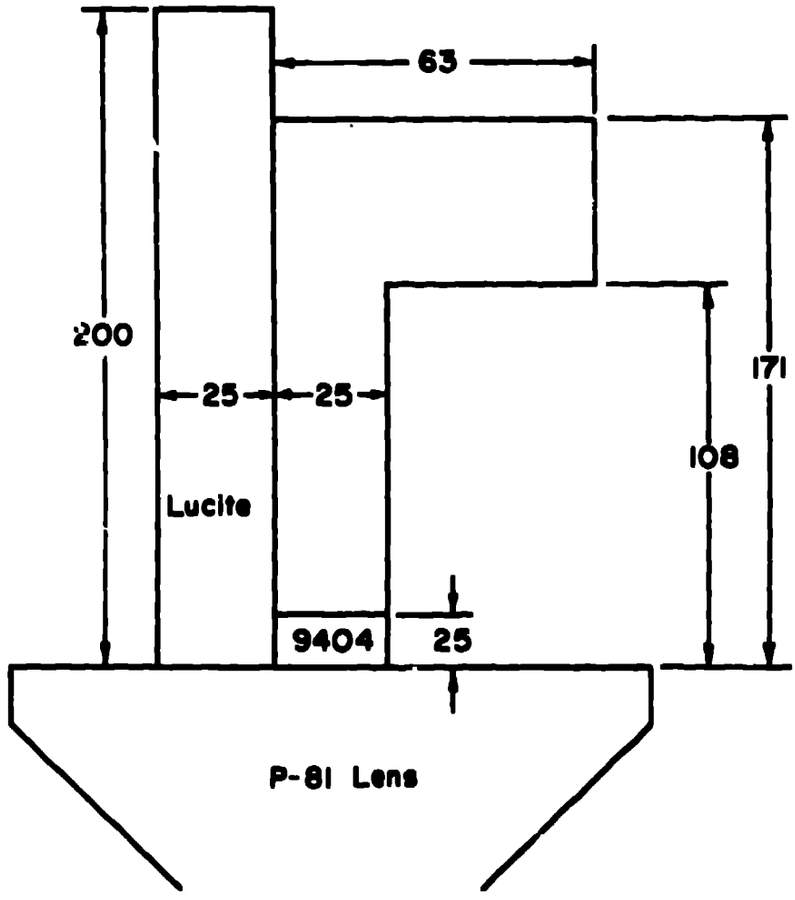

Figure 1

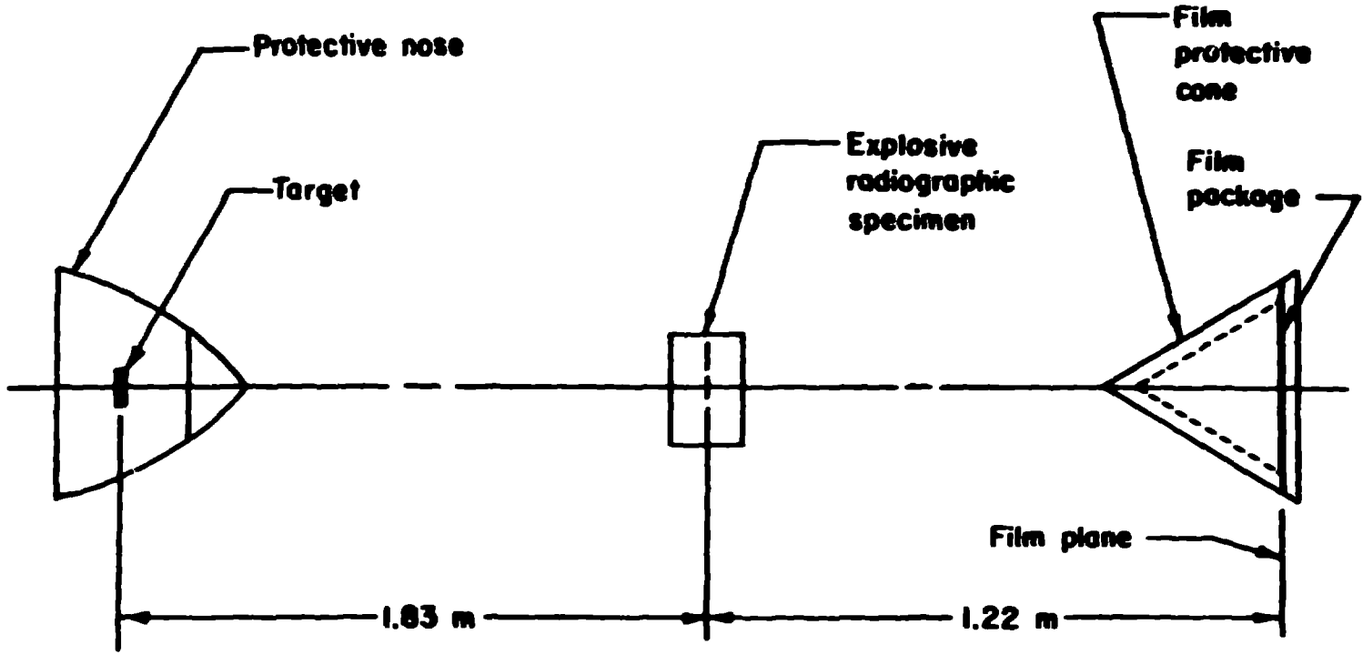
Protective nose
Target
Explosive radiographic specimen
Film protective cone
Film package
Film plane
1.83 m
1.22 m

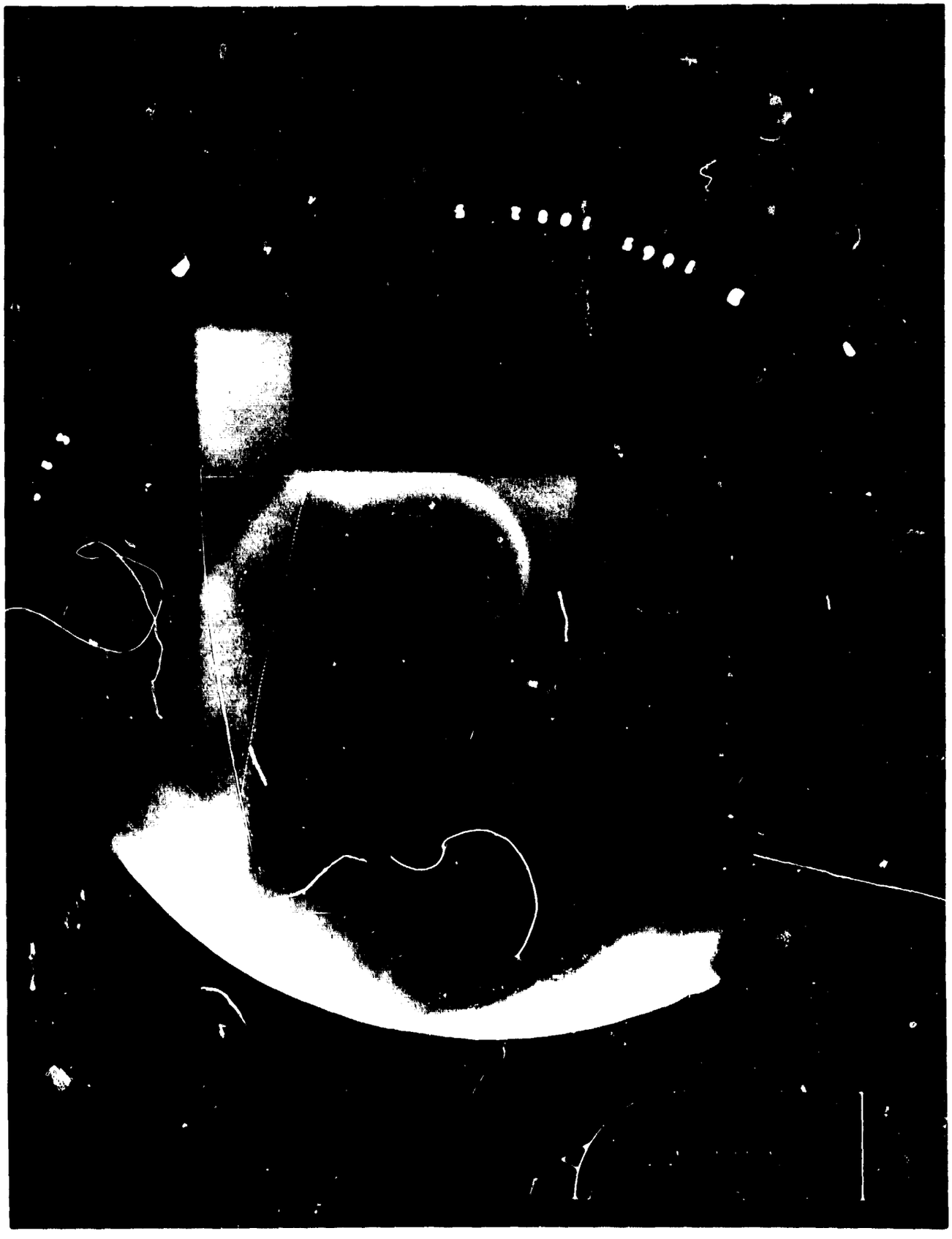

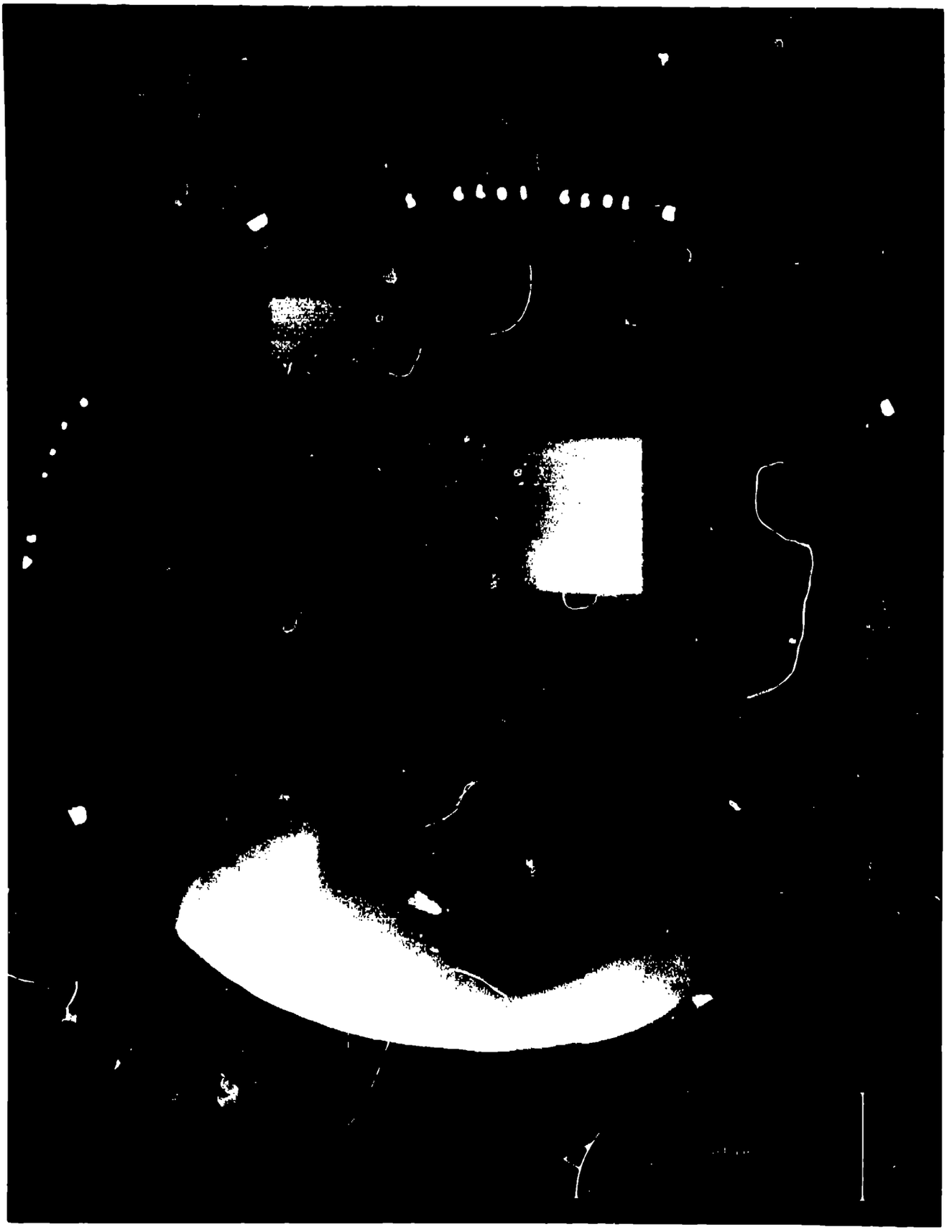

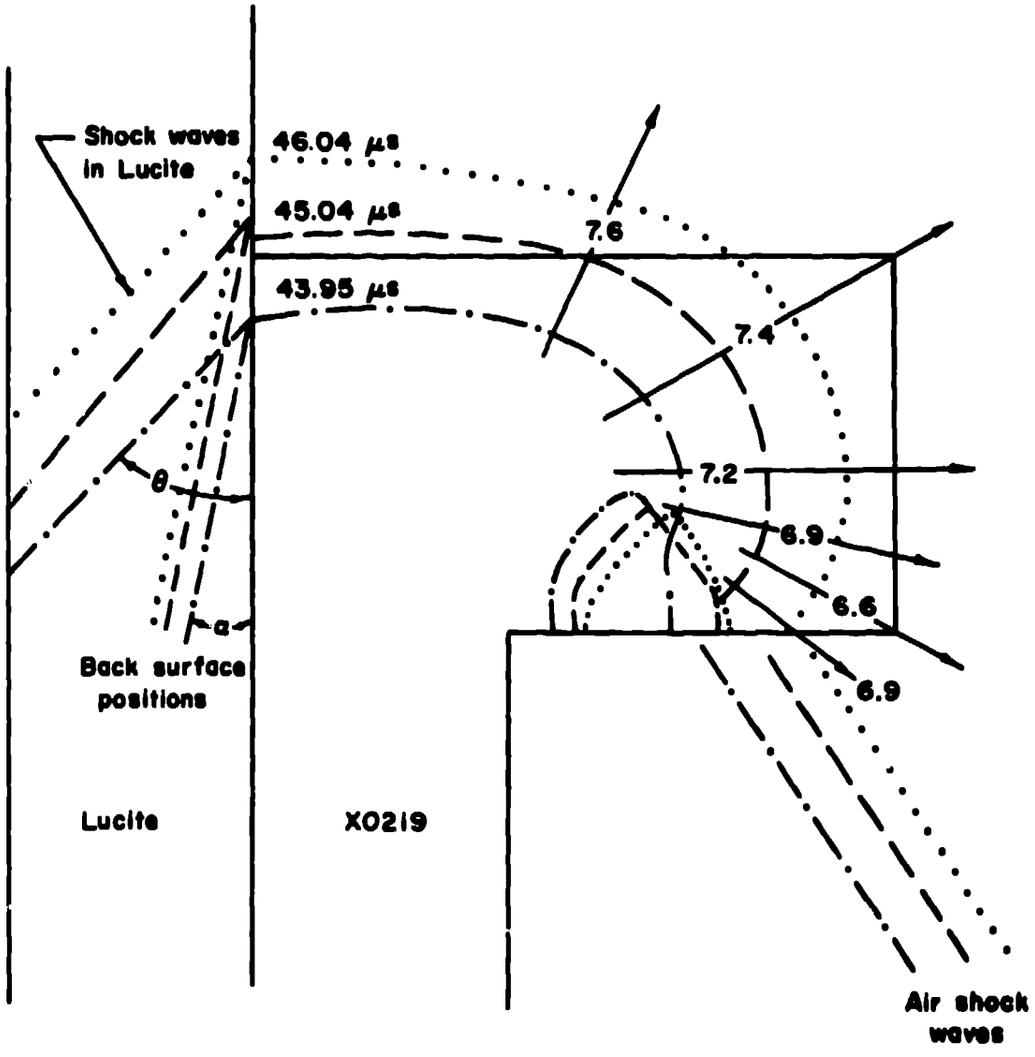
Shock waves in Lucite
46.04 μs
45.04 μs
43.95 μs
7.6
7.4
7.2
6.9
6.6
6.9
θ
α
Back surface positions
Lucite
XO219
Air shock waves

Figure 5

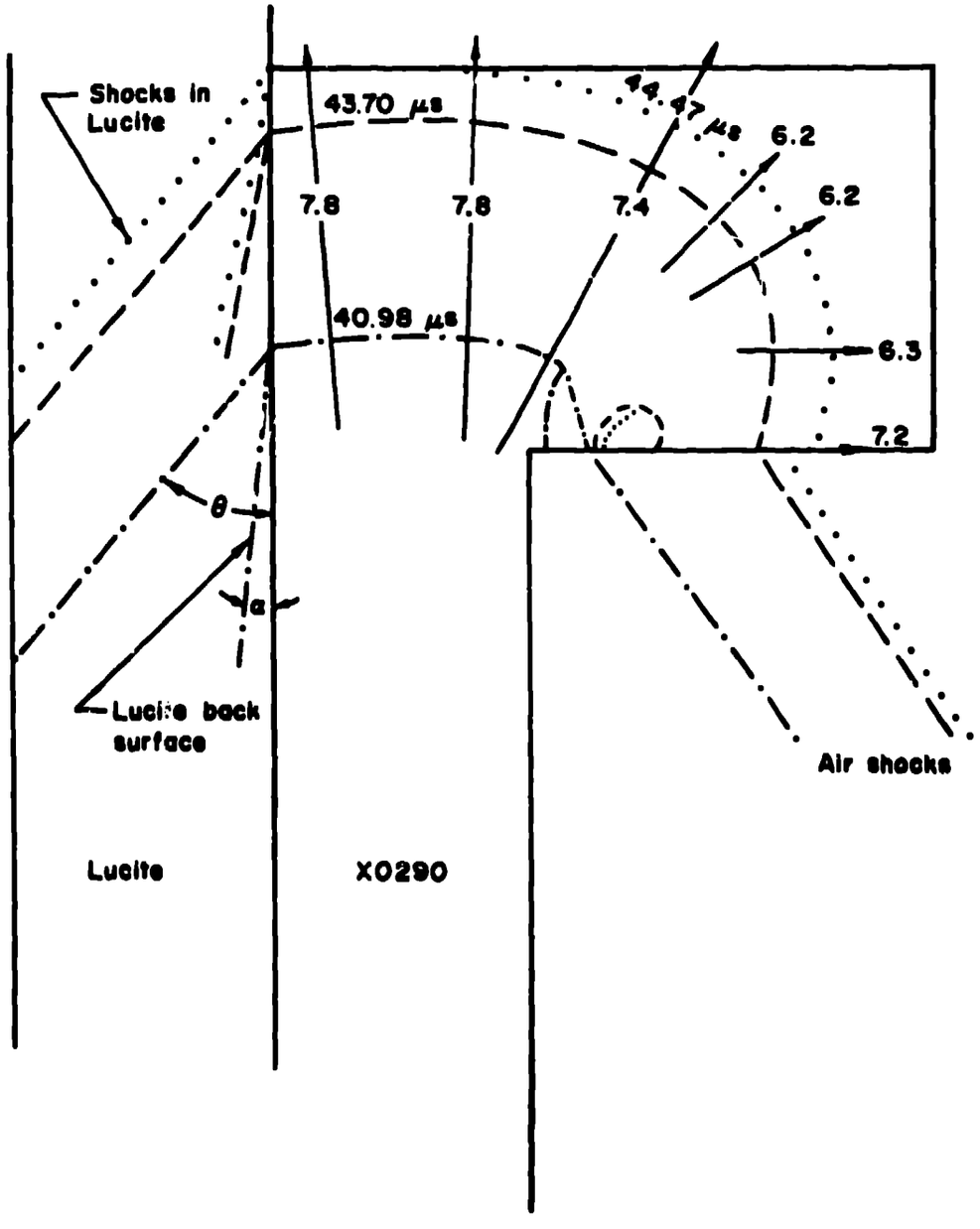
Shocks in Lucite
43.70 μs
44.47 μs
6.2
6.2
7.8
7.8
7.4
40.98 μs
6.3
7.2
θ
α
Lucite back surface
Air shocks
Lucite
X0290

Figure 6

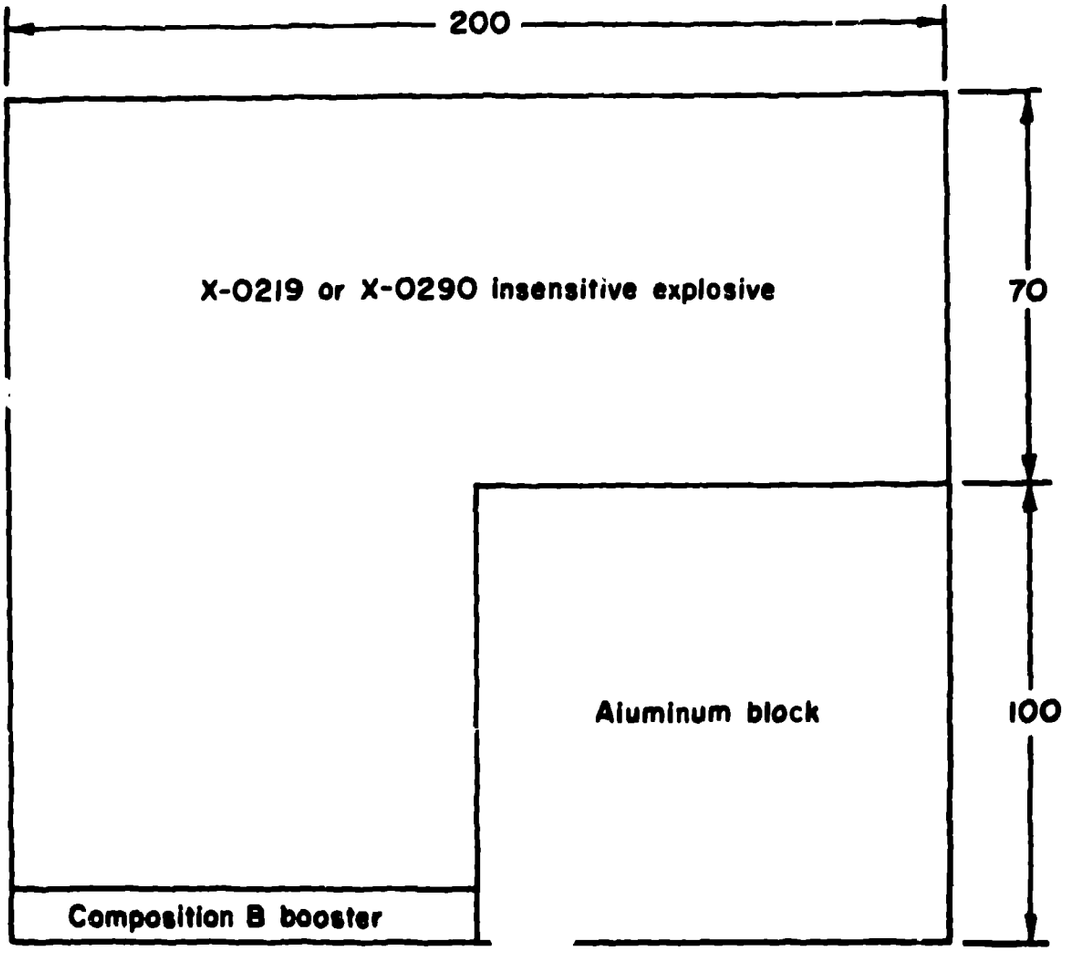
200
X-0219 or X-0290 insensitive explosive
70
Aluminum block
100
Composition B booster

P-81 Lens

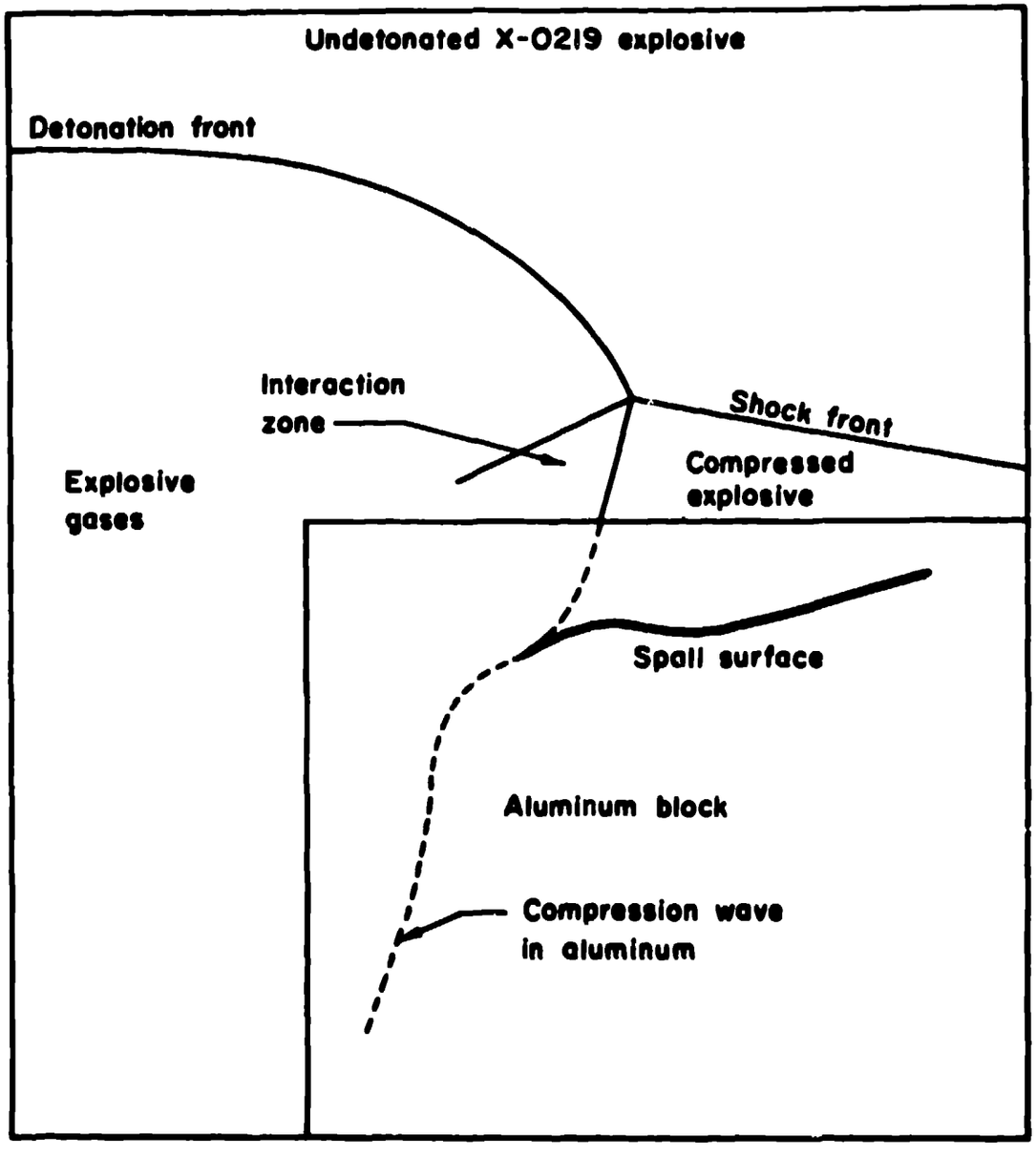
Undetonated X-0219 explosive
Detonation front
Interaction zone
Shock front
Compressed explosive
Explosive gases
Spall surface
Aluminum block
Compression wave in aluminum

Figure 9

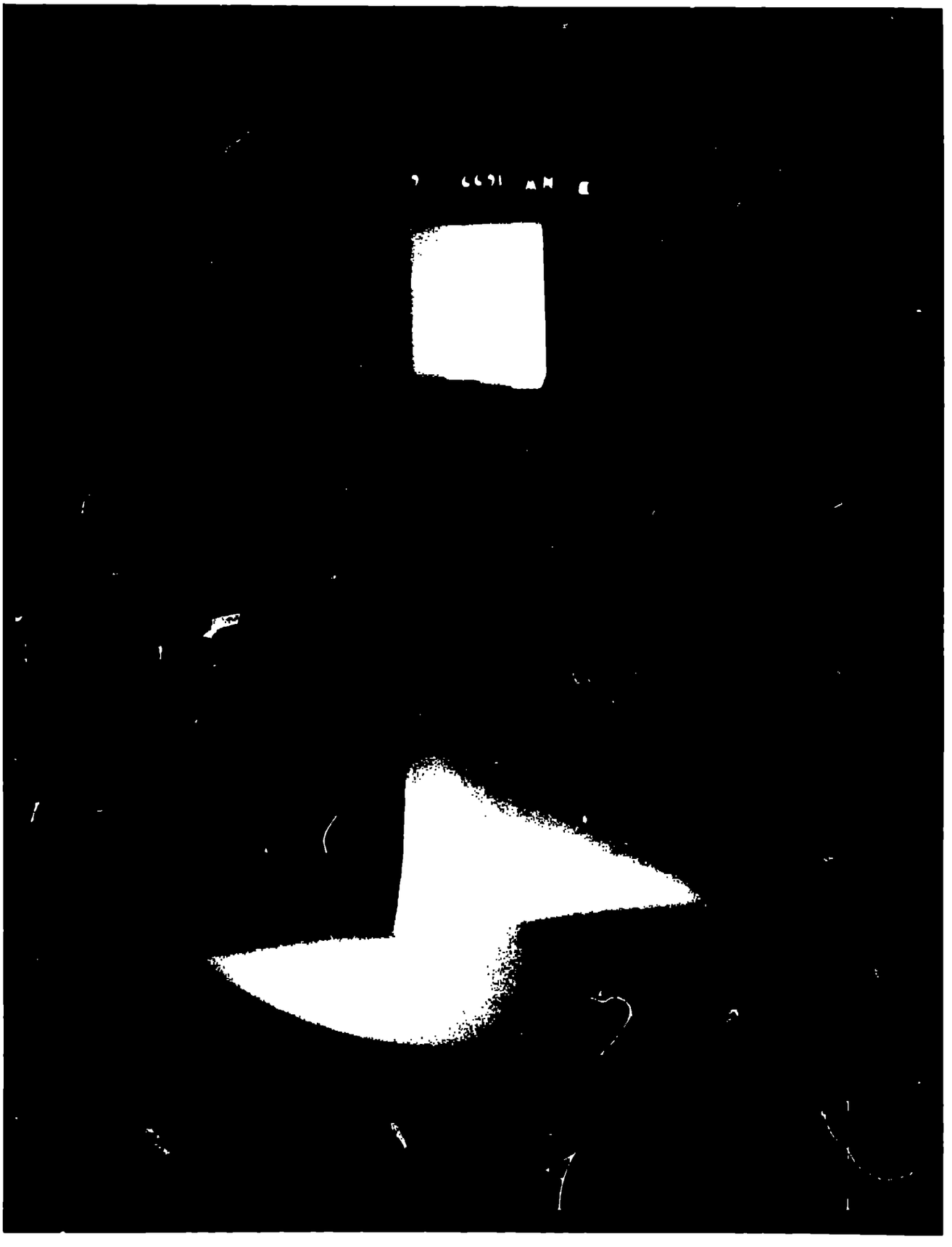

Figure 10

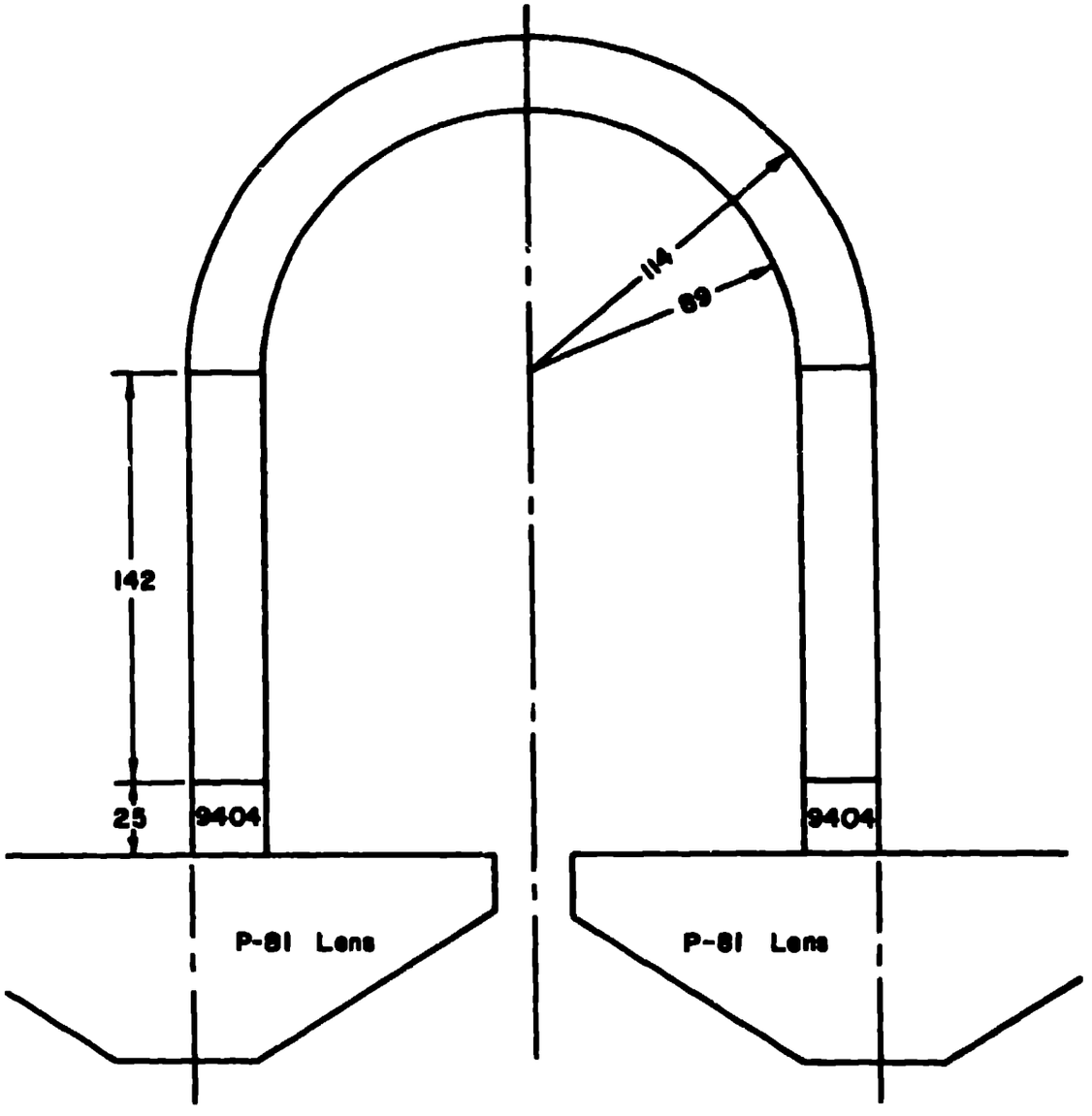

Figure 11

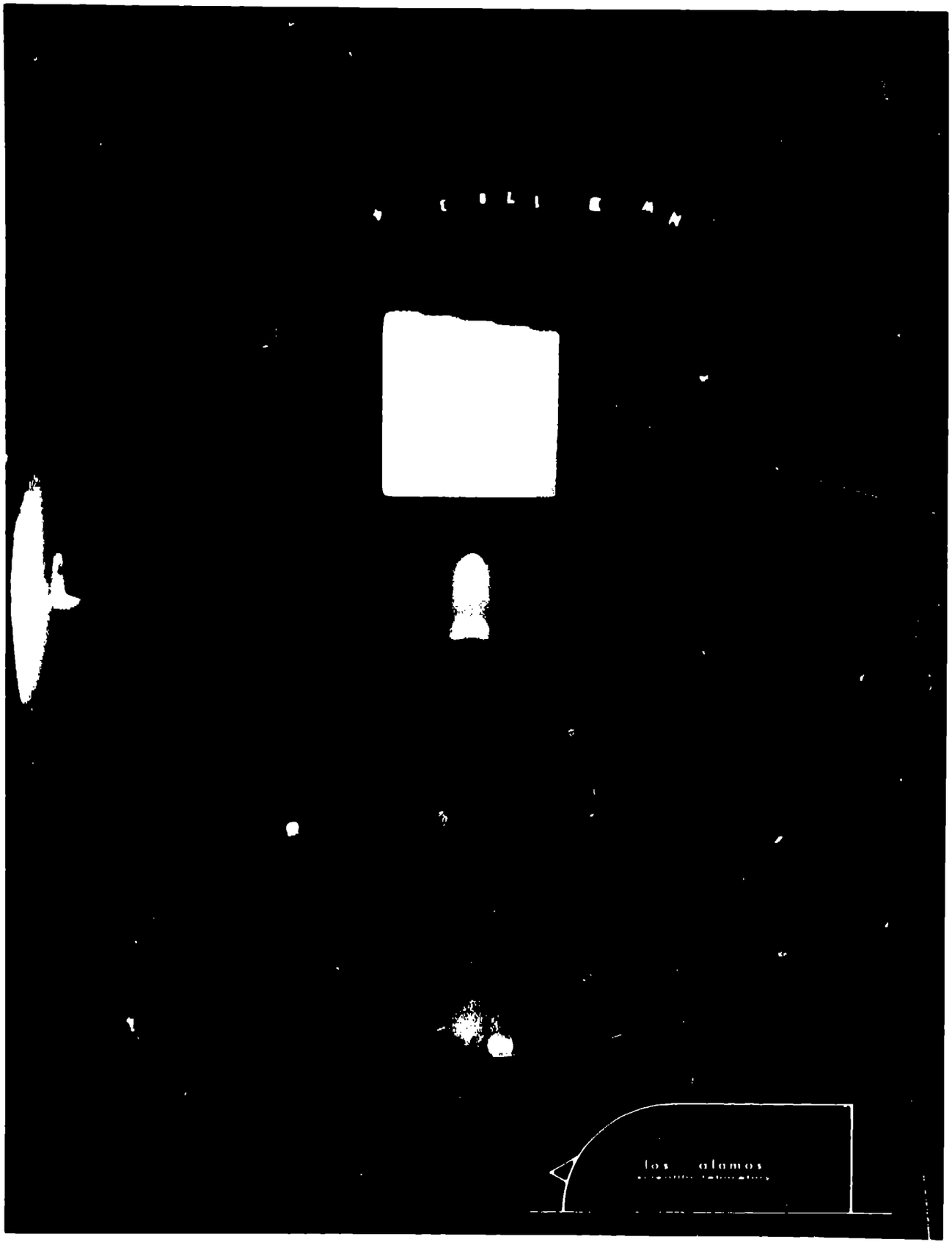

Figure 12

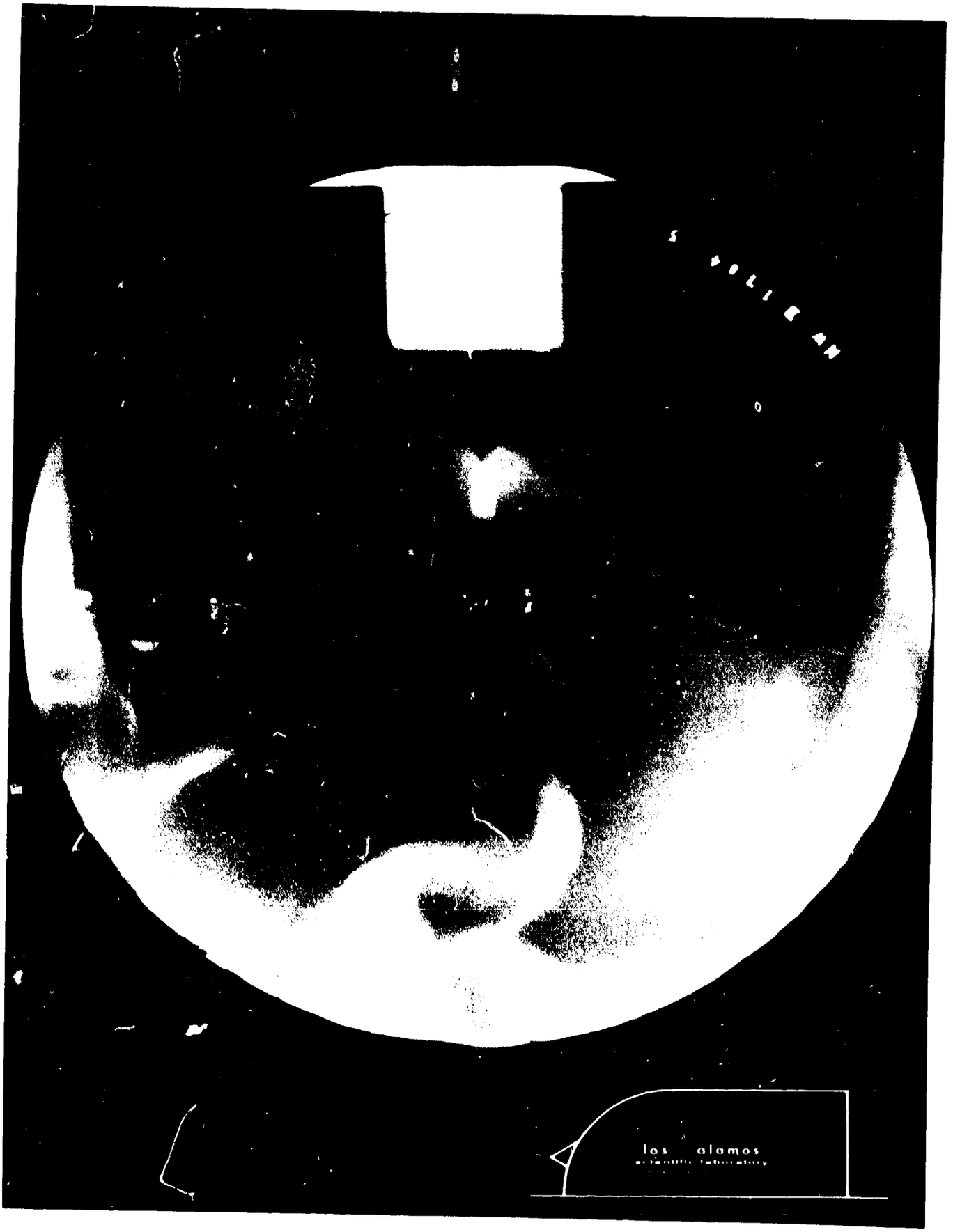
los alamos